Deposition of insoluble calcium phosphate layers by combining finely dispersed calcium hydroxide sols with soluble phosphates

Antonia Tigrano[1*], *Gerald* Ziegenbalg[1]

[1]IBZ-Salzchemie GmbH & Co. KG, 09633 Halsbruecke Germany

Abstract. Carbonate containing materials are subject to severe weathering. Traditional formulations of stone strengtheners have low compatibility with the original material and further they contain VOCs (volatile organic compounds), which endanger human health and the environment.
This study explores the high potential of novel treatments based on water-soluble phosphates used as an agent to react with calcium carbonate ($CaCO_3$) to form an insoluble film of calcium phosphate in the pore space of the treated material. Pretreatments with nanolime suspensions ensure greater availability of calcium ions and reduce the consumption of the original material in the reactions. An alkaline environment is required to promote the conversion of the $CaCO_3$ components to hydroxyapatite-like compounds. Based on experiments in aqueous solutions, different sources of phosphate ions could be examined and compared for the development of effective treatments to apply on different test specimens. To implement the treatments, barium phosphate solutions were investigated. Important aspects of this research are the use of green solvents and the search of components that avoid the formation of byproducts, to increase the efficiency of the chemical reactions and reduce possible negative effects on the operator, the environment and the very same built heritage material.
The developed treatments are a valuable alternative to the traditional methods, as it follows an improvement in the material properties without affecting the moisture transport within it and allows the evenly reaction of the strengthened material to external physical and mechanical stresses without creating internal tension between the grains.

1 Introduction

Preserving materials that represent our cultural heritage is a complex challenge. A variety of factors such as material properties, type and intensity of damage, degradation mechanisms, and specific environmental conditions must be taken into account when addressing the problem, defining the necessary actions, and selecting materials or processes.

It is therefore necessary to select and develop appropriate means and methods for correct conservation treatment, because each intervention must be considered unique and planned

*Corresponding author: antonia.tigrano@ibz-freiberg.de

These proceedings are published with the support of EuLA.

specifically for the object in question. Consolidation can be risky because its effects can be irreversible and undesirable.

Porous carbonate materials are found in both historic and modern buildings. Strengthening them is a recurring task. Traditionally, organic and inorganic consolidation products have been used to restore the original mechanical properties of weathered and damaged materials, but their compatibility and durability on the original substrate are often critical. Traditional consolidation products include lime water, calcium hydroxide grouts, cement paste, sodium silicate and resins. Problems with their application are: coarse particle size, low penetration, high hardness or hydrophobicity of the newly formed structures, incompatible physicochemical and sometimes limited durability. For this reason, the use of inorganic nanomaterial-based consolidation products for architectural heritage preservation has increased significantly in recent years. Nanoparticles can penetrate deep into the damaged historic fabric and are highly compatible with the original substrate: the newly formed phases must be able to seal the microcracks between the stone grains without completely filling the pore space. They improve the material properties without affecting the moisture transfer in the building material. The nanometric particles have a larger specific surface area than in conventional suspensions. This increases their chemical reactivity and significantly improves material properties. In particular, this category includes strengthening agents based on calcium or magnesium hydroxide nanoparticles ($Ca(OH)_2$ and $Mg(OH)_2$), which are used to strengthen carbonate rocks such as limestone or dolomite and mortars [1-9]. Barium hydroxide nanosuspensions ($Ba(OH)_2$) or solutions are widely used for the fixation of soluble sulfates and for the consolidation of wall paintings [5, 44, 45]. The treatment method is based on the Ferroni-Dini process [25, 26]. Nanosuspensions of strontium hydroxide ($Sr(OH)_2$) have also been proposed for similar applications [27]. Nanosuspensions of silica (SiO_2 sol, silica sol, colloidal silica) are also used for stone strengthening, but these have the tendency to form xerogels on the surface of the stone, therefore only a low penetration depth can be achieved [1]. As an alternative, silicic acid esters (SAE) are widely used. The most commonly used products are based on tetraethyl orthosilicate (TEOS). The resulting silica gel is characterized by a graded polarity that preserves the capillarity and water vapor permeability of the original material. However, silica esters cannot be used when large voids or cracks are present because they are unable to bridge them [1, 5].

In this study, alternative novel treatments based on nanosuspensions of calcium hydroxide in combination with soluble phosphates were developed and evaluated, not only for the purpose of strengthening, but also to apply a protective treatment that allows the nucleation and growth of a layer composed by insoluble calcium phosphate (CaP) over the original and/or newly formed surfaces in the pore space, so that the dissolution of the carbonate substrate due to weathering processes, can be reduced or avoided. The effectiveness of CaP layers is based on their low solubility in water and their lattice compatibility with calcite. This allows these materials to respond uniformly to external physical and mechanical stresses without generating internal stresses.

The high potential of phosphate treatment has been described in many publications [29-36]. The authors proposed the use of water-soluble phosphates as an active agent to react with $CaCO_3$ in limestone, marble, carbonate-bonded sandstones and also archaeological bones to form hydroxyapatite (HAP) in the pore space of the treated material. The use of diammonium hydrogen phosphate (DAHP) is considered to be particularly effective as it leads to the formation of ammonium ions (NH_4^+) and hydrogen phosphate ions (HPO_4^{2-}) in aqueous solution.

In this paper, the treatment with DAHP has been compared with the implementation of nanolime (CaLoSiL®E25) pretreatments and the formed phases were characterized chemically. The drying and setting time after the application of CaLoSiL® was studied in order to obtain a homogeneous, uniformly distributed protective layer of nano- or

microcrystals of insoluble calcium phosphate. It was therefore necessary to ensure a gradual evaporation of the solvent and also to provide the necessary atmosphere for the reactions to take place in the pore solution. High humidity conditions for several days favor the reaction and the crystallinity of the newly formed material.

Barium phosphate solutions have also been developed for the same purpose. The aim of the treatment was to obtain a high pH in the pore solution and, consequently, apatite phases rich in calcium. The advantage of using such precursors is that only chemicals that are completely used in the reaction are introduced, resulting in higher efficiency without the formation of by-products. An additional problem in consolidation operations is that substrates are often contaminated by the presence of salts. Treatment with barium phosphate solution results in at least partial conversion of soluble sulfates to insoluble $BaSO_4$, while the simultaneous presence of Ca^{2+} leads to the formation of insoluble calcium phosphates, which may also incorporate sulfate and barium ions into their crystalline lattice.

To verify that the application of the later solution results in the formation of insoluble phases, the samples were eluted in deionized water and a quantitative chemical analysis was performed on the filtrate.

2 Chemistry of the calcium phosphate

Calcium orthophosphates (CaP) are salts of trivalent phosphoric acid H_3PO_4 and form compounds that can contain phosphate anions at a different protonation state (PO_4^{3-}, HPO_4^{2-} and $H_2PO_4^{-}$). The three dissociation stages of the orthophosphate system and their acid dissociation constant pK_a (at 25 °C) are given in equations 1 to 3 [23]:

$$H_3PO_4 \rightleftharpoons H^+ + H_2PO_4^- \quad pK_1 = 2{,}16 \qquad (1)$$
$$H_2PO_4^- \rightleftharpoons H^+ + HPO_4^{2-} \quad pK_2 = 7{,}21 \qquad (2)$$
$$HPO_4^{2-} \rightleftharpoons H^+ + PO_4^{3-} \quad pK_3 = 12{,}32 \qquad (3)$$

All calcium phosphates are white crystalline solids that are slightly soluble in water. Some CaP contain water of crystallization, such as dicalcium phosphate dihydrate (DCPD or brushite) and octacalcium phosphate (OCP), others can incorporate OH^- ions into their lattice. The last belong to the apatite group. The crystallization of complex, insoluble apatite occurs by intermediate precipitation of metastable precursors in accordance with Ostwald's step rule [51]. The apatite compounds are among the preferred phases formed under neutral to basic conditions. During precipitation reactions in a basic environment, amorphous calcium phosphate (ACP) and OCP are often formed as intermediates, as they are the kinetically preferred phases that convert to the thermodynamically more stable hydroxyapatite in subsequent steps [11-14]. The molar Ca/P ratio and the solubility in water are the most important parameters for the differentiation of CaP. In general, the lower the molar Ca/P ratio, the more acidic and water soluble the compound. Table 1 lists the major members of the CaP family that are of interest to this study. It is important to emphasize that for the purpose of this study, only the method of preparation of CaP by wet-chemical precipitation at room temperature has been considered [41].

Stoichiometric hydroxyapatite is the least soluble and therefore most stable calcium orthophosphate and is generally described by the chemical formula $Ca_{10}(PO_4)_6(OH)_2$. It cannot be obtained by direct precipitation in aqueous solutions at room temperature in presence of atmospheric CO_2. The particularity of HAP lattice is that its hexagonal structure is particularly susceptible to defects and foreign ions. Substitutions can occur at various lattice sites, resulting in a wide variety of compounds.

CDHA (calcium deficient HAP) is easily prepared by precipitation in an aqueous basic solution. Due to the non-stoichiometric nature of CDHA, it contains a proportion of foreign ions at calcium and hydroxyl positions. Construction errors are also known in anion positions:

phosphate ions may be partially protonated ($Ca_{10-x}(HPO_4)_x(PO_4)_{6-x}(OH)_{2-x}$ with $0 < x < 1$) and partially replaced by carbonate ions (CO_3^{2-}). OH^- or PO_4^{3-} can be replaced by CO_3^{2-} ions in HAP lattices, resulting in carbonate-hydroxyapatite (CHAP) of type A or B. In the first case, a CO_3^{2-} ion replaces two OH^- ions in the lattice, which is described by the chemical formula $Ca_{10}(PO_4)_6(OH)_{2-2y}(CO_3)_y$ where $0 \leq y \leq 1$. In the second case, the substitution of CO_3^{2-} takes place at the phosphate position. Electroneutrality is maintained by substitution also at the cation position. This compound is described by the formula $Ca_{10-x}M_x(PO_4)_{6-x}(CO_3)_x(OH)_2$ where $0 \leq x \leq 2$ and M = monovalent cation (e.g. Na^+, K^+). During the precipitation of HAP in aqueous solutions, both types of substitutions can occur simultaneously, resulting in a mixed AB-type hydroxyapatite with the formula $Ca_{10}[(PO_4)_{6-x}(CO_3)_x][(OH)_{2-y}(CO_3)_y]$ [15, 16]. Substitution of monovalent or divalent cations can always take place at the cation position, as well as substitutions of other types of anions such as SO_4^{2-}, SiO_4^{4-}, Cl^-, etc. The formation of substituted HAP ($0 < x \leq 2$) can be described by the equation 4:

$$(10-x)Ca^{2+} + xHPO_4{}^{2-} + (6-x)PO_4{}^{3-} + (2-x)OH^- \rightarrow Ca_{10-x}(HPO_4)_x(PO_4)_{6-x}(OH)_{2-x} \quad (4)$$

Table 1. Properties and thermodynamics of some calcium phosphates compared to calcite [14, 17].

Name	Ca/P molar ratio	-lgKs (at 25 °C)	pH stability range (in H_2O at 25 °C)	ΔG^0 [kJ mol-1]
HAP	1.67	116,8	9,5 - 12	-12.68
CDHA	1.5-1.67	85,1	6,5 – 9,5	[a]
CHAP	> 1.67 (depending on CO_3^{2-} content)	depending on CO_3^{2-} content	7 - 12	[a]
OCP	1.33	96,6	5,5 – 7	-12.26
ACP	1.2-2.2	25 – 33	5-12	[b]
DCPD	1,0	6,59	2 – 6	-2.16
Calcite	-	8,5	> 7	-1.13

HAP: hydroxyapatite, **CDHA**: calcium-deficient HAP, **CHAP**: carbonate HAP, **OCP**: octacalcium phosphate; **ACP**: amorphous calcium phosphate; **DCPD**: brushite; [a] no data; [b] metastable.

3 Materials and methods

3.1 Chemicals and reagents

The following chemicals were used: $CaCO_3$ (CHEMSOLUTE, ≥ 99.5%), $(NH_4)_2HPO_4$ (chemPUR, 98+%), CaLoSiL® E25 (IBZ Salzchemie Freiberg, DE), Phenolphthalein (Roth, ≥ 99%), Ethanol, H_3PO_4 (adds4food, 85% E338), $Ba(OH)_2 \cdot 8H_2O$ (Thermo Fisher, 97%). For the preparation of saturated solutions to create a humid environment for the sample storage: technical NaCl and $NaNO_3$ (Roth). For the preparation of saturated solutions for the determination of water transport: LiCl (SuboLab, 99%) and KNO_3 (CHEMSOLUTE, > 99%).

3.2 Prepared solutions for the treatments

For the first treatment, a 1 mol/l aqueous solution of diammonium hydrogen phosphate (DAHP) was prepared. Following are the properties of this solution: pH = 8.15; ρ = 1.07 g/cm^3. In order to follow the pH fluctuations of the reactions in the test samples, a solution of 0,1 wt.% of phenolphthalein in 30 wt.% water, 70 wt.% ethanol was prepared.

For the second treatment, an aqueous suspension of 0.2 mol/l $Ba(OH)_2$ was prepared. This was used to titrate a 0.5 mol/l orthophosphoric acid and obtain a barium phosphate solution with pH = 2.5, ρ = 1.02 g/cm^3.

3.3 Test specimens

3.3.1 Mortar sample characteristics

The prismatic test specimens were prepared in metal molds according to DIN EN 1015-11 - Annex A [38]. These had the dimensions 40 mm x 40 mm x 40 mm or 160 mm x 40 mm x 40 mm, into which a slaked lime/sand mixture was added in a mass ratio of 1:8. Medium-grained sand (0-2 mm) was used. Round test specimens were produced in cut plastic tubes with a diameter of 45 mm, a height of 16 mm and using a lime/sand ratio of 1:8. The mortar was placed in the appropriate molds with only slight pressure to achieve low density and open porosity. This type of sample preparation makes possible to simulate the ageing processes on the materials and to obtain comparable, reproducible results.

3.3.2 Treatments

In principle, the mortar prisms were consolidated by two different treatments. These are shown schematically in Figure 1. The treatments were carried out with slight modifications: different sources of phosphate ions were used, but the technique of application and the final storage conditions were always identical. Table 2 shows the different phosphate solutions used and the number of applications, as well as whether there was a pretreatment with nanolime. In treatment 1, after pretreatment with CaLoSiL® E25, one series of the test specimens were stored for 24 h in laboratory and then treated with the phosphate solution. Another series of prisms, after nanolime pretreatment, were stored 14 d in a controlled humid environment at RH = 70-75% to ensure that carbonating occurs. The carbonation reaction as well as the reaction to calcium phosphate was followed by dripping a small drop of the phenolphthalein solution on each lateral side of the prisms. After the phosphate solution application, the specimens were stored in the same humid environment at RH = 70-75% and T = 20-22 °C until constant weight was reached. The samples were weighed before and after each treatment step. This made it possible to determine the mass of the reinforcing agent that had penetrated and the final increase in mass.

Before performing treatment 2, the test specimens were stored for 2 hours in a 0.3 mol/l $MgSO_4$ solution. The barium phosphate treatment was carried out after the sample lost ca. 90% of the water content and stored after treatment in the same condition as the previous described treatments.

After treatment 2, the samples were ground in a mortar, stirred for 4 h in deionized water and slow filtered. The soluble fraction over insoluble was determined by weighing the filter cakes. The filtrate was prepared for the chemical analysis.

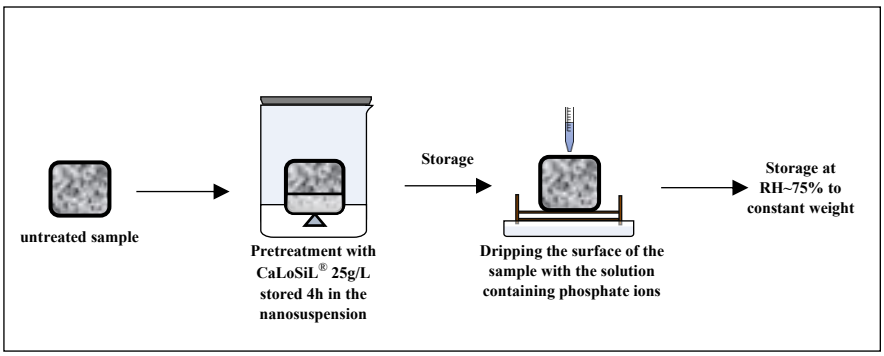

Fig. 1. General schematic representation of the treatments carried out on the test specimens.

Table 2. Treatments and number of applications for each treatment.

Treatment	CaLoSiL® E25	Storage	DAHP	Ba-phosphate
1a			1 application	
1b	1 application	24h, laboratory	1 application	
1c	1 application	14d, RH ~ 70%	1 application	
2-1		2h in a 0.3 mol/l $MgSO_4$ solution, 24h, laboratory		1 application
2-2				2 applications

3.4 Materials characterization

The strengthening effect was verified by determining a variety of physical, mechanical and microstructural properties, as well as durability tests based on capillary water absorption [39], water vapor permeability [40], longitudinal wave ultrasonic velocity (performed with the Geotron electronic measuring system, using the LightHouse UMPC software) and compressive strength (performed using the Inspekt Desk 10 kN measurement system and the LabMaster software) [38]. In addition, structural studies were performed using X-ray powder diffraction (XRD). An XRD 3003 TT with energy dispersive detector Meteor0D (GE Inspection Technologies), which is equipped with a Θ - Θ goniometer, was used for this purpose. The diffraction patterns were recorded with Cu-Kα radiation in the measurement range of 10° to 80° Θ with a resolution of 0.02° Θ per second. The compounds were identified using Analyze software and the ICDD database. Scanning electron microscopy (SEM) was used to characterize the microstructures formed in the pore spaces. Measurements were acquired on a Jeol JSM-7001F SEM (high vacuum, accelerated voltage: 5 kV), which generates high-resolution images with secondary electron contrast (SE) of the uneven object surface. Furthermore, the elemental composition of individual formed structures was analyzed via energy dispersive X-ray analysis (SEM-EDX). An EDX detector Bruker e⁻-Flash was used (high vacuum, accelerated voltage: 15 kV). The highly porous samples were mounted on a Cu-Zn sample carrier, the uneven edges were filled with a graphite containing adhesive and finally carbon was vapor deposited. A silver coating on the edges helped to increase the conductivity of the samples.

Changes in mass and color of the treated mortar prisms were also followed and characterized. The colorimetric analysis was performed using a Precision Colorimeter NR20XE from 3nh and evaluated with the CQCS3 software.

For the quantitative determination of an analyte were used different methods. The chemical analysis was conducted by gravimetric analysis for the determination of the SO_4^{2-} content, by photometric measurements (at 712 nm) for the determination of the PO_4^{3-} and ICP-OES was used to determine the content of Ca^{2+}, Ba^{2+}, Mg^{2+}, Na^{+}, K^{+}.

4 Results and discussion

4.1 Treatment with CaLoSiL® and DAHP solution

The treatments carried out resulted in an average increase in mass of 1 wt% for all the samples treated with 1 mol/l DAHP solution (treatment 1a), 1.2 wt% for the samples treated with CaLoSiL® and DAHP solution with drying time of 24 hours in laboratory (treatment 1b) and 2.4 wt% for those treated with CaLoSiL® and DAHP solution after a single application, with a curing time of 14 days at RH ~ 70% between the two procedures (treatment 1c). The prisms

treated with treatment 1b did not show significant results and improvements compared to the material after the treatment 1a, therefore are not discussed in the results.

Table 3 shows the results of the mechanical/physical properties tests of the treated materials compared to the same untreated material. The determination of the compressive strength of the mortar prisms of treatment 1a and 1c after 28 days gave very good results. The tests on the specimens clearly showed that the material properties improved significantly compared to the untreated material. The sample pretreated with nanolime generally showed the higher coefficient values. In addition, a significant increase in ultrasonic velocity was also achieved. As a non-destructive characterization method, it can be used in studies on original materials where compressive strength cannot be used because it destroys the specimens. The validity of ultrasonic testing has been demonstrated by the consistency of the results obtained.

The hydrophilic behavior of the test specimens was maintained with only minor impairment of capillary water transport. The water absorption coefficient (*C*) deviates only about 15% after treatment 1c, suggesting that the pores are slightly more filled than after treatment 1a. A similar picture emerges for the effect on water vapor permeability (W_{vp}): there are no significant changes in either the lower or upper range.

The visual observations were supplemented by colorimetric measurements of the samples before and after the treatments. The color difference ΔE^* can vary greatly due to the general inhomogeneity of the mortar prisms. To reduce this effect, a mask was used to position the colorimeter on the same measuring point. The least superficial whitening was observed in treatment 1c. In general, this color change is barely noticeable to the human eye [37].

Table 3. Determined mechanical and physical properties of untreated and treated specimens.

Treatment	Compressive strength [N/mm²]	Ultrasonic velocity [m/s]	*C* [kg/m² h$^{0.5}$]	W_{vp} lower range [kg/m s Pa]	W_{vp} upper range [kg/m s Pa]	ΔE^*
untreated	0.6 ± 0.1	1645 ± 130	1.7 ± 0.1	2.9E-11 ± 2E-12	5.2E-11 ± 4E-12	
1a	1.1 ± 0.3	2469 ± 174	1.7 ± 0.01	2.7E-11 ± 8E-12	5.3E-11 ± 4E-12	1.8 ± 0.2
1c	2.1 ± 0.3	3444 ± 370	1.4 ± 0.1	2.4E-11 ± 3E-12	5.3E-11 ± 2E-12	1.5 ± 0.8

All results shown are expressed as value ± standard deviation, n=3, except W_{vp}, where n=5; ***C***: water absorption coefficient; W_{vp}: water vapor permeability; ΔE^*: color difference

Based on information from preliminary stirring tests, the reaction to CaP generally takes up to 6 hours to form ACP, which later converts to the crystalline phase. The longer the storage time, the higher the crystallinity of the product. With SEM observation, it was possible to observe and define the phases obtained. In Figure 2 is shown the morphology of the layers formed and Figure 3 the EDX measurement points carried out to identify the compounds formed by elemental quantitative analysis. Compared to the untreated samples, the treatments resulted in a coverage of the surface with different density and uniformity, no cracks were found in the protective film. Treatment 1a showed an uneven coverage. The carbonate matrix does not differ significantly from the reference samples and does not have any particular crystalline forms. This may indicate the presence of a deposition layer of ACP on the original substrate that is very low in phosphorus and therefore phosphate content (Figure 3). It should be pointed out that in quantitative analysis the contribution of carbon from the deposition layer of graphite must be taken into account. This can be up to 10 at% in a spot analysis.

Treatment 1c, on the other hand, resulted in the formation of a homogeneous, evenly distributed layer of microcrystals distributed over the entire sample with the same composition (Figure 4a). Thanks to the pretreatment with CaLoSiL®, the formation of crystalline phases of calcium phosphate was observed: this can be found as CHAP or CDHA in form of porous “petal like” aggregates and non-stoichiometric platelets. OCP

modifications are also not to exclude, since it is an intermediate of the reaction. The molar Ca/P ratio is strongly influenced by the presence of substitutions on the part of CO_3^{2-} in the lattice. Additionally, the presence Mg^{2+} incorporated into the lattice led to the formation of micrometric prismatic crystals (Figure 4b) observed throughout the sample. Other platelets containing additional zinc were found. However, this did not affect the homogeneity of the protective film. Unfortunately, there is no way to completely prevent such reactions. The metal ions Mg^{2+}, Zn^{2+}, and traces Na^{+}, K^{+}, Fe^{2+} (below 1 at%), come from the sand or impurities in the binder of the mortar samples.

The analysis of the diffraction pattern of the binder portion of a sample mortar after treatment 1c (gently ground and sieved to 90 µm) is shown in Figure 5. Here, the calcite and hydroxyapatite reflexes could be assigned. The reflexes in the range of 22-26° (002-reflexes of stoichiometric HAP) are not very intense and the reflexes in the range of 32-34° (211-reflexes of stoichiometric HAP) are significantly wide, indicating that the formed phases contain crystallographic defects caused by substitution in anionic and cationic position in the HAP lattice.

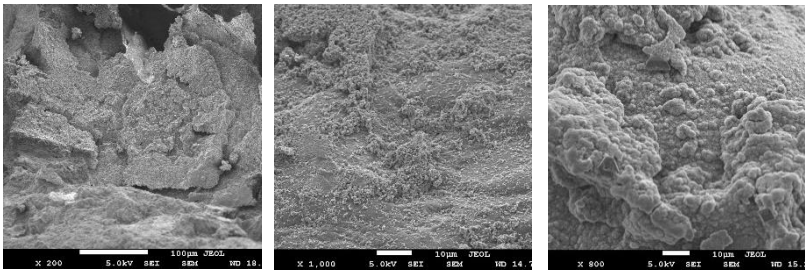

Fig. 2. SEM images of the untreated sample (left), after treatment 1a (center) and after treatment 1c (right).

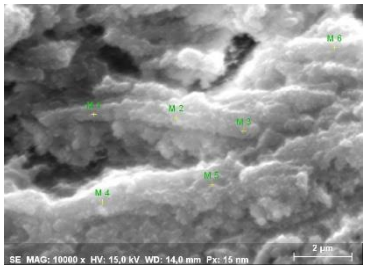

Spektrum	C	O	P	Ca	Ca/P
M 1	25.9	52.2	4.3	15.9	3.7
M 2	27.3	51.9	4.2	15.1	3.6
M 3	29.9	50.3	3.6	14.8	4.1
M 4	25.1	54.7	2.9	15.8	5.5
M 5	27.9	53.7	2.8	14.3	5.1
M 6	30.5	51.4	4.3	12.3	2.9

Fig. 3. SEM images and elemental analysis on a sample after treatment with a 1 mol/l DAHP solution (treatment 1a). The results are given in atomic percentage (at%). The uncertainty of the analysis is shown in Figure 8.

(a)

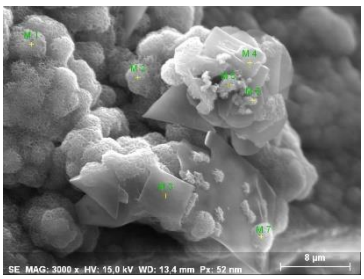

Spektrum	C	O	Mg	P	Ca	Ca/P
M 1	27.5	55.9		5.1	10.5	2.04
M 2	27.8	54.4		5.9	10.9	1.83
M 3	30.3	52.2	3.6	6.5	6.7	
M 4	41.1	46.0		4.8	5.9	1.24
M 5	27.5	48.6	5.2	9.6	6.6	
M 6	37.4	45.6	2.2	6.7	5.2	
M 7	27.4	42.8		8.8	20.7	2.34

(b)

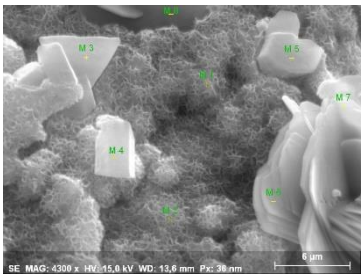

Spektrum	C	O	Mg	Zn	P	Ca	Ca/P
M 1	22.2	57.7			6.1	13.0	2.15
M 2	22.0	59.4			5.8	11.9	2.07
M 3	27.9	55.7	3.3		5.6	6.5	
M 4	32.0	51.9	4.4		6.0	4.9	
M 5	28.4	55.3	4.3		5.5	5.7	
M 6	26.5	51.7		2.3	7.2	9.7	
M 7	29.3	51.5		2.1	5.4	10.4	
M8	19.2	56,7			7.4	13.3	1.81

Fig. 4. SEM images and EDX elemental analysis on different spots in a sample after a treatment with CaLoSiL® and a 1 mol/l DAHP solution (treatment 1c). The results are given in atomic percentage (at%). The uncertainty of the analysis is shown in Figure 8.

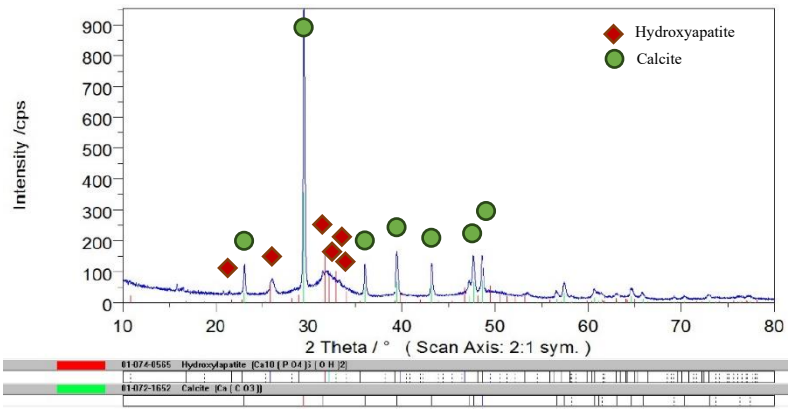

Fig. 5. XRD pattern of a sample after a treatment with CaLoSiL® and a 1 mol/l DAHP solution (treatment 1c).

4.2 Treatment with barium phosphate solution

Table 4 presents the average in ion content of the samples after one and two applications of the treatment solution. In comparison with the results obtained after dissolving the samples, it can be seen that soluble sulphates were still present. The barium and phosphate ions were stably converted to insoluble compounds, as was magnesium, that can react to $Mg(OH)_2$ and after carbonation, in $MgCO_3$, or form double salts. Sulphates present are not completely converted into insoluble compounds, but already almost half of the content could be fixed in insoluble phases after one application. The total change in mass of the samples could not be determined accurately because it is affected by the amount of salt contamination and moisture content due to the presence of hygroscopic salts.

Both treatments had very little effect on the color of the original material. A color difference ΔE^* of 1.8 ± 0.3 (value ± standard deviation, n=3) was measured after one application of the barium phosphate treatment and a ΔE^* of 1.6 ± 0.6 after two applications of the same treatment, which is barely noticeable to the human eye.

The determination of the compressive strength of the mortar prisms after only a week after the second application of the barium phosphate solution was carried out to determine if there was already an increase in value even though the samples were not completely dry. The conducted test proved that the mechanical properties improved adequately compared to the untreated material already after 7 days of the treatment: values of 0.4 ± 0.04 N/mm^2 (value ± standard deviation, n=3) were measured in comparison to the untreated material with a compressive strength of 0.2 ± 0.04 N/mm^2.

Table 4. Theoretical ion content calculated from the absorbed phosphate solution and results of the quantitative chemical analysis on analytes after stirring the samples in deionized water.

Theoretical ion content after:	**Ca^{2+} wt%**	**Ba^{2+} wt%**	**Mg^{2+} wt%**	**SO_4^{2-} wt%**	**PO_4^{3-} wt%**	**pH**	**LF [mS/cm]**
1 application		0.3	0.2	0.9	0.6	-	-
2 applications		0.5			1.1		
Ion content after samples elution:							
1 application	0.1	0.0	0.05	0.5	0.0	8.8	2.9
2 applications	0.1	0.0	0.02	0.4	0.0	9.1	2.5

Figure 6 shows and compares the structures formed after the treatments carried out. It is easy to observe how the application of a second treatment makes the coating more homogeneous and distributed over the carbonate matrix and the sand grains. The quantitative SEM-EDX analysis revealed the formation of mixed $Ca^{2+}/Ba^{2+}/Mg^{2+}$ and PO_4^{3-}/SO_4^{2-} phases. However, the crystallinity of these phases is very low (Fig. 7) and no crystals of defined shape are present. A second treatment, therefore a larger supply of phosphate ions, leads to the separation of a highly crystalline phase, enriched in calcium and phosphate content, with a Ca/P molar ratio very close to 1.67 (Fig. 8), which means that the conditions imposed by the initial pH of the given solution, time and reaction conditions are very favorable and have led to the formation of non-stoichiometric apatite, but with minimal substitution in the lattice. At the same time, a great portion of the sulfate ions present were fixed in insoluble phases, that resulted to remain stable from dissolution.

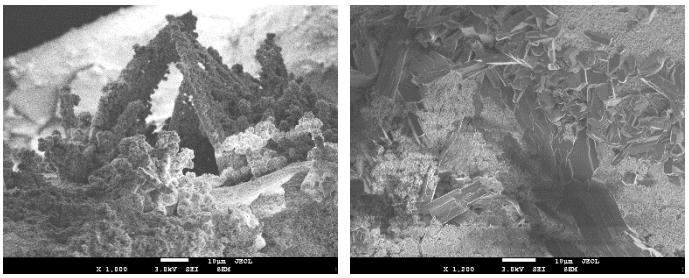

Fig. 6. SEM images of in a sample after one treatment with Ba-PO_4 solution (treatment 2-1, left) and after two treatments with the same solution (treatment 2-2, right).

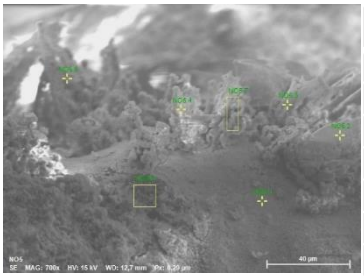

Spektrum	C	O	Mg	P	S	Ca	Ba
NO5_1	14.6	52.3		2.0	2.3	13.3	14.9
NO5_2	13.7	52.0		4.0	3.2	6.2	19.7
NO5_3	10.9	48.2	1.0	5.3	4.2	5.8	24.5
NO5_4	10.9	47.1		4.4	4.0	6.7	25.9
NO5_5	9.4	44.0	1.0	5.4	3.7	5.3	31.0
NO5_6	15.2	55.5				23.4	
NO5_7	9.6	45.5	1.1	5.4	4.3	6.3	27.8

Fig. 7. SEM images and EDX elemental analysis in a sample after one treatment with Ba-PO_4 solution. The results are given in atomic percentage (at%). The uncertainty of the analysis is shown in Figure 8.

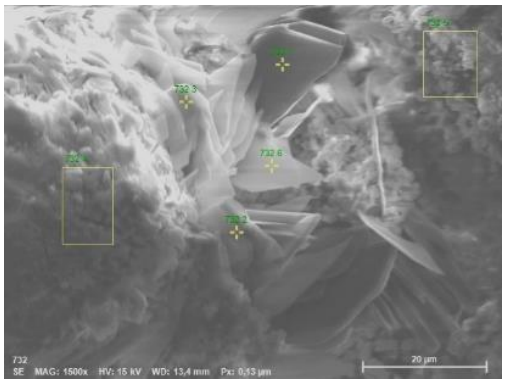

Spektrum	C	O	Mg	P	S	Ca	Ba	Ca/P
732_1	6.2 ± 0.6	49.3 ± 3.4		17.0 ± 0.4		27.5 ± 0.5		1.61
732_2	8.9 ± 0.8	52.5 ± 3.4		14.0 ± 0.3	1.2 ± 0.03	21.4 ± 0.3	1.7 ± 0.01	1.52
732_3	12.3 ± 1.0	56.1 ± 3.4		10.6 ± 0.2	1.5 ± 0.03	17.1 ± 0.3	2.0 ± 0.01	1.61
732_4	14.1 ± 1.1	56.6 ± 3.4	2.3 ± 0.1	5.7 ± 0.1	3.5 ± 0.1	9.0 ± 0.1	8.5 ± 0.1	
732_5	9.1 ± 0.9	47.0 ± 3.4	2.3 ± 0.1	5.0 ± 0.1	6.5 ± 0.2	5.0 ± 0.1	25.0 ± 0.1	
732_6	11.6 ± 1.0	54.4 ± 3.4		10.7 ± 0.2	1.6 ± 0.04	15.8 ± 0.2	5.3 ± 0.03	1.47

Fig. 8. SEM images and EDX elemental analysis in a sample after two treatments with Ba-PO_4 solution. The results are given in atomic percentage (at% ± 1σ).

5 Conclusion

All the studies carried out have shown that apatite formation requires a variety of different preconditions. Studies and treatments have been developed to ensure that chemically neutral components can be formed in practical applications. In addition, the use of hazardous solvents for the operator and the environment was completely avoided.

The tests to develop a protective treatment for carbonate materials included DAHP as a source of phosphate ions and gave excellent results. DAHP solutions have a low viscosity and can penetrate deep into the substrate undergoing consolidation. Pretreatment with nanolime is very helpful as the original substrate is only slightly exposed to the phosphate solution. Partial carbonation as a result of nanolime treatment is beneficial for the production of crystalline products. A homogeneous, evenly distributed protective layer of microcrystals of carbonate HAP with a high calcium content is formed. Their formation is facilitated by a sufficient amount of Ca^{2+} and PO_4^{3-}: the $CaCO_3$ particle surface supplies the overlying aqueous phosphate solution with Ca^{2+} ions. Hydrogen phosphate and phosphate ions can freely migrate to the reaction site. The primary crystals grow together during the subsequent

storage period to form petal-like crystals of carbonate hydroxyapatite (CHAP) and platelets of very high crystallinity. Long storage times in a humid environment and the use of higher pH values in the reaction mixture favored the crystallization of insoluble CaP. Moreover, the presence of residual $Ca(OH)_2$ after CaLoSiL® application supported the achievement of an alkaline environment, which is essential for apatite formation. There was minimal transport of solid particles back to the surface of the samples during solvent evaporation, resulting in an imperceptible change in surface color. The subsequent partial filling of the pore space caused by the secondary mineral formation led to an improvement in the material properties and caused only a minimal slowing of water transport in the test materials.

The use of this method should be considered on a case-by-case basis. The ammonium ions provided by the dissociation of DAHP could lead to the precipitation of ammonium carbonate, a water-soluble salt. By using a 1 mol/l DAHP solution in the treatment described, the presence of this salt was not detected. In the treatments carried out, ammonia should be formed as a gaseous component in the reaction solution and released completely. This would be a minor disadvantage of the DAHP process. Treatment of outdoor objects is very effective if appropriate personal protection measures are taken. The use of this method indoors is more problematic. A system of air filters for NH_3 fixation and air exchange is required.

On the other hand, the use of barium phosphate solutions avoids completely this problem. The composition of this solution has been carefully tested to achieve an initial pH in solution as high as possible, without the introduction of additional bases other than barium hydroxide to avoid providing further ions that may react to form unwanted products.

When the solution is applied to the material, the ions present react with the substrate, to form apatite-like bonds. The dissolution of the $CaCO_3$ present and the subsequent reaction of the calcium ions leads to the establishment of a pH in solution in the neutral-alkaline zone, resulting in the precipitation of new, more pure, insoluble mineral phases of CaP or apatite, with high crystallinity, characterized by only few substitutions in the crystal lattice. The new phases formed by the application of these two alternative sources of phosphate ions are stable upon dissolution, providing consolidation and protection to the material over long periods of time.

The use of a solution containing barium and phosphate ions was developed to expand the potential of the phosphate treatment and treat also materials that are contaminated by the presence of salts, in particular soluble sulfates. Overall, a treatment with a barium phosphate solution is considered to be promising. The solution is compatible with the base material and penetrates well. The use of barium phosphate solutions not only fixes the sulphate ions, but also solidifies the material, which is also indicated by the fact that the test samples remain compact when touched. In order to achieve a crystalline protective film, long-term consolidation or sulphate fixation, the material should be treated at least twice.

The authors thank Kathrin Bruemmer for the contribution in the execution of the preliminary tests on solutions, Kerstin Schmieder and Dorothee Schwalbe of IBZ-Salzchemie for their assistance with the quantitative chemical analysis. We would also like to thank Anja Obst of the SEM facility at TUBAF (Freiberg) for the SEM images and EDX measurements and Dr. Udo Steiner of the XRD facility at HTWD (Dresden) for the XRD measurements.

References

1. A. Sierra-Fernández, L.S. Gómez Villalba, M.E. Rabanal, R. Fort González, New nanomaterials for applications in conservation and restoration of stony materials: A review. Materiales de Construcción **67**, 107 (2017). https://doi.org/10.3989/mc.2017.07616

2. S.Papatzani, E. Dimitrakakis, A review of the assessment tools for the efficiency of nanolime calcareous stone consolidant products for historic structures. Buildings **9**, 235 (2019). https://doi.org/10.3390/buildings9110235
3. Ö.Cizer, C. Rodriguez-Navarro, E. Ruiz-Agudo, J. Elsen, D. Van Gemert, K. Van Balen, Phase and morfology evolution of calcium carbonate precipitated by carbonation of hydrated lime. J Mater Sci **47**, 6151-6165 (2012). https://doi.org/10.1007/s10853-012-6535-7
4. C.Rodriguez-Navarro, K. Elert, R. Ševčík, Amorphous and crystalline calcium carbonate phases during carbonation of nanolimes: implications in heritage conservation. CrystEngComm **18**, 6594-6607 (2016) https://doi.org/10.1007/s10853-012-6535-7
5. G. Ziegenbalg, M. Drdácký, C. Dietze, D. Schuch, Nanomaterials in Architecture and Art Conservation (Pan Stanford Publishing, 2018)
6. G. Ziegenbalg, M. Dobrzyńska-Musiela, Nanolime – possible applications for the conservation and protection of the cultural heritage, in Euro-American Congress Rehabend, Burgos, Spain, May 24-27 (2016)
7. E. Maryniak-Piaszczynski, G. Ziegenbalg, Nanolime as a binder for injection grouts and repair mortars, in Historic Mortars - HMC 2010 and RILEM TC 203-RHM final workshop, Prag (2010), 1301-1309
8. G. Ziegenbalg, Colloidal calcium hydroxide – a new material for consolidation and conservation of carbonatic stones, in Proceedings of the 11th International Congress on Deterioration and Conservation of Stone, Torun (2008), 1109-1115
9. P. Baglioni, R. Giorgi, Soft and hard nanomaterials for restoration and conservation of cultural heritage. Soft Matter **2**, 293-303 (2006) https://doi.org/10.1039/b516442g
10. D. Chelazzi, R. Giorgi, L. Dei, P. Baglioni, Nanotecnologie per la conservazione del patrimonio culturale. La Chimica e l'industria **10**, 78-82 (2005)
11. E. Hayek, H. Newesely, W. Hassenteufel, B. Krismer, Zur Bildungsweise und Morfologie der schwerlöslichen Calciumphosphate. Mh. Chem. Bd. **91**, 249–262 (1960) https://doi.org/10.1007/BF00901743
12. S. Chander, D. W. Fuerstenau, Interfacial Properties and Equilibria in the Apatite-Aqueous Solution System. Journal of Colloid and Interface Science **70(3)**, 506-516 (1979) https://doi.org/10.1016/0021-9797(79)90058-4
13. O. Mekmene, S. Quillard, T. Rouillon, J. M. Bouler, M. Piot, F. Gaucheron, Effects of pH and Ca/P molar ratio on the quantity and crystalline structure of calcium phosphates obtained from aqueous solutions. Dairy Science & Technology **89(3)**, 301-316 (2009) https://doi.org/10.1051/dst/2009019
14. C. Drouet, A comprehensive guide to experimental and predicted thermodynamic properties of phosphate apatite minerals in view of applicative purposes. J. Chem. Thermodynamics **81**, 143-159 (2015) https://doi.org/10.1016/j.jct.2014.09.012
15. I.R. Gibson, W. Bonfield, Novel synthesis and characterization of an AB-type carbonate-substituted hydroxyapatite. Journal of Biomedical Materials Research **59 (4)**, 697-708 (2002) https://doi.org/10.1002/jbm.10044
16. S.A. Siddiqi, U. Azhar, Carbonate substituted hydroxyapatite, in Woodhead Publishing Series in Biomaterials, Handbook of Ionic Substituted Hydroxyapatites, 149-173 (Woodhead Publishing, 2020) https://doi.org/10.1016/B978-0-08-102834-6.00006-9

17. M. Epple, S.V. Dorozhkin, Die biologische und medizinische Bedeutung von Calciumphosphaten. Angew. Chem. **114**, 3260-3277 (2002) https://doi.org/10.1002/1521-3757(20020902)114:17<3260::AID-ANGE3260>3.0.CO;2-S
18. J.E. Harries, D.W.L. Hukins, C. Holt, S.S. Hasnain, Conversion of amorphous calcium phosphate into hydroxyapatite investigated by EXAFS spectroscopy. Journal of Crystal Growth **84(4)**, 563-570 (1987) https://doi.org/10.1016/0022-0248(87)90046-7
19. M.S. Tung, T.J. O'Farrell, Effect of ethanol on the formation of calcium phosphates. Colloids Surfaces A: Physicochem. Eng. Aspects **110**, 191-198 (1996) https://doi.org/10.1016/0927-7757(95)03450-1
20. S. Naidu, G.W. Scherer, Nucleation, growth and evolution of calcium phosphate films on calcite. Journal of Colloid and Interface Science **435**, 128-137 (2014) https://doi.org/10.1016/j.jcis.2014.08.018
21. Z. Zhuang, H. Yamamoto, M. Aizawa, Synthesis of plate-shaped hydroxyapatite via an enzyme reaction of urea with urease and is characterization. Powder Technology **222**, 193-200 (2012) https://doi.org/10.1016/j.powtec.2012.02.046
22. M. Iijima, K. Onuma, Particle-size-dependent octacalcium phosphate overgrowth on β-tricalcium phosphate substrate in calcium phosphate solution. Ceramics International **44(2)** (2017) https://doi.org/10.1016/j.ceramint.2017.10.167
23. E. Wiberg, A.F. Holleman, Lehrbuch der anorganischen Chemie. 90. Aufl. (de Gruyter, Berlin, 1976) 731-734
24. E. Ferroni, Atti del Convegno Internazionale di Studi 'Piero della Francesca ad Arezzo', Arezzo, Italy, March 7-10 (1990)
25. E. Ferroni, Il contributo delle scienze chimiche per la conoscenza e la conservazione preventiva. OPD Restauro **11**, 97-102 (1999)
26. M. Licchelli, M. Malagodi, M. Weththimuni, C. Zanchi, Nanoparticles for conservation of bio-calcarenite stone. Applied Physics A: Materials Science & Processing **114**, 673-683 (2013) https://doi.org/10.1007/s00339-013-7973-z
27. B. Gonçalves, C. Southwick, Sustainability in Conservation for South America: Turning to Green Conservation for the Preservation of Culture Heritage. Contributions from Speakers **40**, 61 (2018)
28. F.P. Byrne, S. Jin, G. Paggiola, T.H.M. Petchey, J.H. Clark, T.J. Farmer, A.J. Hunt, R.C. McElroy, J. Sherwood, Tools and techniques for solvent selection: green solvent selection guides. Sustain Chem Process **4(7)**, 1-24 (2016) https://doi.org/10.1186/s40508-016-0051-z
29. E. Sassoni, G. Graziani, E. Franzoni, An innovative phosphate-based consolidant for limestone. Part 1: Effectiveness and compatibility in comparison with ethyl silicate. Construction and Building Materials **102**, 918-930 (2016) https://doi.org/10.1016/j.conbuildmat.2015.04.026
30. E. Sassoni, Phosphate-based treatments for conservation of stone. RILEM Technical Letters **2**, 14-19 (2017) https://doi.org/10.21809/rilemtechlett.2017.34
31. M. Matteini, S. Rescic, F. Fratini, G. Botticelli, Ammonium Phosphates as Consolidating Agents for Carbonatic Stone Materials Used in Architecture and Cultural Heritage: Preliminary Research. Conservation, Analysis and Restoration **5(6)**, 717-736 (2011) https://doi.org/10.1080/15583058.2010.495445

32. A. Shekofteh, E. Molina, L. Rueda-Quero, A. Arizzi, G. Cultrone, The efficiency of nanolime and dibasic ammonium phosphate in the consolidation of beige limestone from the Pasargadae World Heritage Site. Archaeol Anthropol Sci **11**, 5065–5080 (2019) https://doi.org/10.1007/s12520-019-00863-y
33. E. Sassoni, Hydroxyapatite and other calcium phosphates for the conservation of cultural heritage: A review. Materials **11(4)**, 557 (2018) https://doi.org/10.3390/ma11040557
34. A. Salvatore, S. Vai, S. Caporali, D. Caramelli, M. Lari, E.Carretti, Evaluation of Diammonium hydrogen phosphate and $Ca(OH)_2$ nanoparticles for consolidation of ancient bones. Journal of Cultural Heritage **41**, 1-12 (2020) https://doi.org/10.1016/j.culher.2019.07.022
35. E. Nesseri, S.C. Boyatzis, N. Boukos, G. Panagiaris, Optimizing the biomimetic synthesis of hydroxyapatite for the consolidation of bone using diammonium phosphate, simulated body fluid, and gelatin. SN Appl. Sci. **2**, 1892 (2020) https://doi.org/10.1007/s42452-020-03547-8
36. A. North, M. Balonis, I. Kakoulli, Biomimetic hydroxyapatite as a new consolidating agent for archaeological bone. Studies in Conservation **61(3)**,146-159 (2016) https://doi.org/10.1179/2047058415Y.0000000020
37. W.S. Mokrzycki, M. Tatol, M. Colour difference ΔE – A survey. Machine Graphics and Vision **20(4)**, 383-411 (2011)
38. DIN EN 1015-11, Prüfverfahren für Mörtel für Mauerwerk – Teil 11: Bestimmung der Biegezug- und Druckfestigkeit von Festmörtel; Deutsche Fassung EN 1015-11:1999+A1:2006
39. DIN EN 1015-18, Prüfverfahren für Mörtel für Mauerwerk – Teil 18: Bestimmung der kapillaren Wasseraufnahme von erhärtetem Mörtel (Festmörtel); Deutsche Fassung EN 1015-18:2002
40. DIN EN 1015-19, Prüfverfahren für Mörtel für Mauerwerk – Teil 19: Bestimmung der Wasserdampfdurchlässigkeit von Festmörteln aus Putzmörteln; Deutsche Fassung EN 1015-19:1998+A1:2004
41. M.V. Nikolenko, K.V. Vasylenko, V.D. Myrhorodska, A. Kostyniuk, B. Likozar, Synthesis of calcium orthophosphates by chemical precipitation in aqueous solutions: the effect of the acidity, Ca/P molar ratio, and temperature on the phase composition and solubility of precipitates. Processes **8**, 1009 (2020) https://doi.org/10.3390/pr8091009
42. D. Stegemann, B. Raj, A.K. Bhaduri, NDT for Analysis of Microstructures and Mechanical Properties of Metallic Materials, Reference Module in Materials Science and Materials Engineering (2016) https://doi.org/10.1016/B978-0-12-803581-8.03429-9
43. H.L. Alberts, 20 2: Ultrasonic Wave Velocities in Solids: Elastic Properties, Temperature, and Pressure Dependence, in Encyclopedia of Materials: Science and Technology, 1-5 (2002) https://doi.org/10.1016/B0-08-043152-6/01824-6
44. J.D. Rodrigues, A.P. Ferreira Pinto, Laboratory and onsite study of barium hydroxide as a consolidant for high porosity limestones, Journal of Cultural Heritage **19** (2015) https://doi.org/10.1016/j.culher.2015.10.002
45. P.I. Girginova, C. Galacho, R. Veiga, A.S. Silva, A. Candeias, Inorganic nanomaterials for restoration of cultural heritage: synthesis approaches towards nano-consolidants for stone and wall paintings, ChemSusChem **11** (2018) https://doi.org/10.1002/cssc.201801982

46. M.J. Arellano-Jiménez, R. García- García, J. Reyes-Gasga, Synthesis and hydrolysis of octacalcium phosphate and its characterization by electron microscopy and X-Ray diffraction. Journal of Physics and Chemistry of Solids **70**, 390-395 (2009) https://doi.org/10.1016/j.jpcs.2008.11.001
47. Y. Rong, J. Yang, S. Huang, Y. Li, Barium hydroxide nanoparticle-phosphoric acid system for desalination and consolidation of tomb murals, Crystals **12**, 1171 (2022) https://doi.org/10.3390/cryst12081171
48. E. Franzoni, E. Sassoni, G. Graziani, Brushing, poultice or immersion? The role of the application technique on the performance of a novel hydroxyapatite-based consolidating treatment for limestone. Journal of Cultural Heritage **2865**, 1-12 (2014) https://doi.org/10.1016/j.culher.2014.05.009
49. E. Possent, C. Colombo, D. Bersani, M. Bertasa, A. Botteon, C. Conti, P.P. Lottici, M. Realini, New insight on the interaction of diammonium hydrogenphosphate conservation treatment with carbonatic substrates: A multi-analytical approach. Microchemical Journal **127**, 79-86 (2016) https://doi.org/10.1016/j.microc.2016.02.008
50. S. Papatzani, E. Dimitrakakis, A review of the assessment tools for the efficiency of nanolime calcareous stone consolidant products for historic structures. Buildings **9(11),** 235 (2019) https://doi.org/10.3390/buildings9110235
51. W. Ostwald, Studien über die Bildung und Umwandlung fester Körper. 1. Abhandlung: Übersättigung und Überkaltung, in Zeitschrift für Physikalische Chemie (International Journal of Research in Physical Chemistry and Chemical Physics) **22**, 289–330 (1987)